

Article

## Advances in Disaster Modeling, Simulation and Visualization for Sandstorm Risk Management in North China

Zhaohui Lin <sup>1,\*</sup>, Jason K. Levy <sup>2</sup>, Hang Lei <sup>3</sup> and Michelle L. Bell <sup>4</sup>

<sup>1</sup> Institute of Atmospheric Physics, Chinese Academy of Sciences, Beijing 100029, China

<sup>2</sup> L. Douglas Wilder School of Government and Public Affairs, Virginia Commonwealth University, Richmond, VA 23284, USA; E-Mail: jklevy@vcu.edu

<sup>3</sup> Department of Atmospheric Sciences, University of Illinois, Urbana, IL 61801, USA; E-Mail: hanglei2@atmos.uiuc.edu

<sup>4</sup> School of Forestry and Environmental Studies, Yale University, 195 Prospect Street, New Haven, CT 06511, USA; E-Mail: michelle.bell@yale.edu

\* Author to whom correspondence should be addressed; E-Mail: lzh@mail.iap.ac.cn; Tel.: +86-10-8299-5125.

Received: 6 March 2012; in revised form: 11 April 2012 / Accepted: 11 April 2012 /

Published: 8 May 2012

---

**Abstract:** Dust storms in North China result in high concentrations of airborne dust particles, which cause detrimental effects on human health as well as social and economic losses and environmental degradation. To investigate the impact of land surface processes on dust storms, we simulate two dust storm events in North China during spring 2002 using two versions of a dust storm prediction system developed by the Institute for Atmospheric Physics (IAP) in Beijing, China. The primary difference between the IAP Sandstorm Prediction System (IAPS 1.0) and more recent version (IAPS 2.0) is the land surface modeling. IAPS 1.0 is based on the Oregon State University (OSU) land surface model, whereas the latest version of the dust storm prediction (IAPS 2.0) uses NOAH land surface schemes for land surface modeling within a meteorological model, MM5. This work investigates whether the improved land surface modeling affects modeling of sandstorms. It is shown that an integrated sandstorm management system can be used to aid the following tasks: ensure sandstorm monitoring and warning; incorporate weather forecasts; ascertain the risk of a sandstorm disaster; integrate multiple technologies (for example, GIS, remote sensing, and information processing technology); track the progress of the storm in real-time; exhibit flexibility, accuracy and reliability (by using multiple sources of data, including in-situ meteorological observations); and monitor PM<sub>10</sub> and PM<sub>2.5</sub> dust

concentrations in airborne dustfalls. The results indicate that with the new land surface scheme, the simulation of soil moisture is greatly improved, leading to a better estimate of the threshold frictional velocity, a key parameter for the estimating surface dust emissions. In this study, we also discuss specific mechanisms by which land surface processes affect dust storm modeling and make recommendations for further improvements to numerical dust storm simulations.

**Keywords:** remote sensing; dust storm modeling; land surface processes; soil moisture; dust-emission; numerical simulation

---

## 1. Introduction

While sandstorms and subsequent airborne dustfalls are natural phenomena, climate change and land use changes associated with deforestation, agricultural expansion, and urbanization are thought to be associated with the frequency of sandstorms around the world [1–3]. For example, a giant sandstorm (haboob) more than a mile high and driven by 60 miles/h (26.82 m/s) winds recently reduced visibility (to zero at the height of the storm), grounded airplanes, and led to traffic congestion across the Valley of the Sun in Arizona, US. Dust storms occur frequently in the spring in North China, contributing to high concentrations of airborne dust particles. A wealth of scientific literature has demonstrated that airborne dust particles adversely impact human health, cause significant social and economic damages and impair the quality of the atmosphere [4–6].

Specifically, Asian dust storms have been associated with human health effects including mortality [7] and hospital admissions [8–11]. The health impacts of airborne particles with aerodynamic diameter  $\leq 10 \mu\text{m}$  ( $\text{PM}_{10}$ ) in 111 major Chinese cities was estimated at over \$29 million (US) [12]. A survey conducted in Seoul, South Korea found that dust storms are perceived to be one of the most serious health threats and 40% of survey respondents reporting a decline in respiratory health during dust storm events [13].

Animal models have demonstrated links between Asian dust and lung inflammation, heart rate, DNA damage, and blood pressure [14–16]. These dust storm events can adversely affect water and energy resources and biodiversity; and particles carried by dust storms can contain heavy metals and other industrial pollutants [17]. Agriculture can be affected through water resources as well as the loss of soil [18]. Sandstorms have been observed in Asia for millennia [19,20]: intense sandstorms occur in North China when the desert and loess regions of China and Mongolia are eroded by winds that exceed 15 m/s for more than three hours, although winds of only 8 m/s are required to blow sand into the air [21–24]. Accordingly, dusty days typically occur in China and Mongolia for two to four months of the year [21,22]. Heavy surface winds, mechanical turbulence, and frontal lifting can cause dust clouds to move hundreds to thousands of kilometers from their original location [25] while low pressure air flows and the polar front can cause sand particles to rise up 6 km in the air [26]. The long range transport of sandstorms and air pollutants has been documented. For example, sand originating in eastern China has caused airborne dustfalls over other parts of Asia and western North America [27–29]. Some measurements indicate that Asian dust storms are increasing in intensity and frequency [30,31]. High

frequency areas for dust storms include North Africa, the Middle East, Mongolia, and China [32].

Remote sensing is a powerful tool to monitor sandstorms, particularly in regions that are lacking meteorological stations. In particular, the high spatial resolution of the National Oceanic and Atmospheric Administration (NOAA) satellite Advanced Very High Resolution Radiometer (AVHRR) data make it useful for collecting sandstorm data. The following NOAA AVHRR channels are used: a visible channel (channel 1, CH1), a near-infrared channel (CH2), a shortwave infrared channel (CH3a), a mid-infrared channel (CH3b), and two thermal-infrared channels (CH4 and CH5). The NOAA/AVHRR CH1 and CH2 channels (located in the visible and near infrared waveband) are capable of measuring and calculating surface albedo while the thermal infrared CH3, CH4, and CH5 channels are used to capture the surface brightness temperature. Surface meteorological charts are used in tandem with NOAA satellite images to measure sandstorms and dustfalls that travel with synoptic-scale air movements. False color composite images are often created in order to monitor the movement of dust clouds and dust particles [21,22,27,33–36].

While geo-stationary meteorological satellites, such as the Visible and Infrared Spin Scan Radiometer (VISSR), operate as part of the GMS-5 satellite system have a lower spatial resolution than NOAA/AVHRR, they can cover the Earth's full disc every 30 min. The visible channel of GMS-5/VISSR is capable of identifying sandstorms, lakes, oceans, ground surfaces, and other targets characterized by low albedo values (calculating the albedo accurately requires corrections due to the angle of depression). Ideally, an integrated sandstorm management system should be able to carry out the following tasks: ensure sandstorm monitoring and warning; incorporate weather forecasts, ascertain the risk of a sandstorm disaster; integrate multiple technologies (for example, geographic information system (GIS), remote sensing, and information processing technology), track the progress of the storm in real-time; exhibit flexibility, accuracy and reliability (by using multiple sources of data, including in-situ meteorological observations); and monitor concentrations of  $PM_{10}$  and particulate matter with aerodynamic diameter  $\leq 2.5 \mu m$  ( $PM_{2.5}$ ) dust concentrations in airborne dustfalls.

There exists a strong need to better understand and predict dust storms and their impacts [17,30,31]. In recent years, extensive research on dust storms has been conducted, including work on dust monitoring [37–40], dust storm frequency analysis [41–43], and simulation and prediction of dust emissions and transportation processes [44–50]. A large literature exists dealing with the numerical simulations of sand storm events in China [51]. Dust emission modeling involves the simulation of synoptic processes, land surface conditions (e.g. soil moisture and soil temperature), and transportation processes as well as the parameterization of wind erosion threshold friction velocity ( $u_{*t}^*$ ) and friction velocity ( $u^*$ ). A land surface model (LSM) can be used to determine land surface properties, including soil moisture. In general,  $u^*$  is dependent on the structure of the atmospheric boundary layer while  $u_{*t}^*$  depends on the land surface characteristics, and land surface model is considered as key component for the dust storm modeling and prediction.

To better understand the impact of land surface processes on dust storm simulations, we modeled the northeast Asian dust storms in the spring of 2002 with two versions of a dust storm numerical modeling and prediction system developed at the Institute for Atmospheric Physics. The two versions of the modeling system, referred to as IAPS 1.0 and IAPS 2.0, differ in their land surface model. In IAPS 1.0 [52], the Oregon State University (OSU) LSM [53,54] is used while in IAPS 2.0 the NOAH LSM [55] is used. The NOAH model was developed by multiple organizations: the National Centers

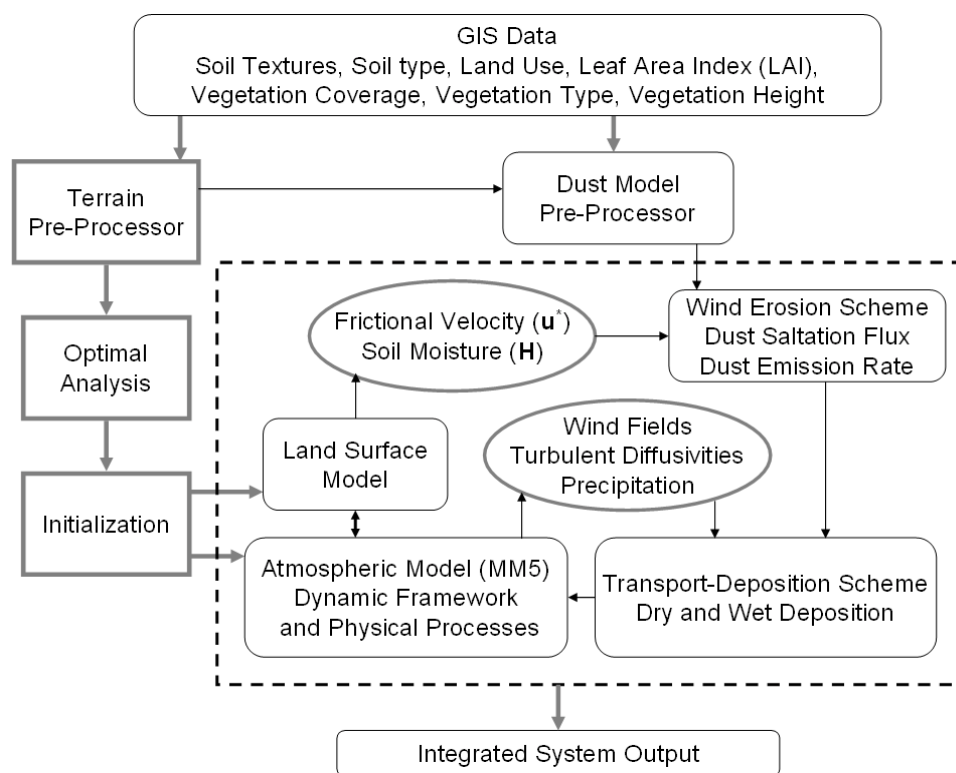
for Environmental Prediction; Oregon State University Department of Atmospheric Sciences; Air Force; and Hydrologic Research Lab of the National Weather Service.

In this paper, results derived from these two different land surface models are compared, and the mechanisms by which land surface processes impact simulated dust storms are investigated. Finally, recommendations are provided for further extending these dust storm modeling systems.

## 2. IAP Dust Storm Simulation and Prediction System (IAPS)

IAPS 1.0 consists of the Meso-scale Meteorological Model (MM5) jointly developed by Pennsylvania State University (PSU) and National Center for Atmospheric Research [56], together with OSU LSM, a wind erosion model, a dust transportation-deposition scheme, pre-processor system, and a GIS database (Figure 1). The pre-processor components include a wind erosion model, dust transportation model and a GIS database with categories for vegetation, soil, and land use. Data generated through the pre-processor components are input into the land surface model, MM5, and wind erosion and dust transportation models. The meteorological model, wind erosion, and dust transportation models are tightly integrated. At each time step  $u^*$  (from the planetary boundary layer scheme) and surface soil moisture (from the land surface scheme) are used by the wind erosion model to calculate the dust emission rate for six particle-size groups. The dust transport and deposition scheme considers advection, diffusion, and dry deposition based on the domain and grid specifications of the MM5 model.

**Figure 1.** The structure of the integrated dust storm numerical modeling systems: dashed lines represent the structure of the Institute for Atmospheric Physics, Dust Storm Simulation and Prediction System (IAPS) model.



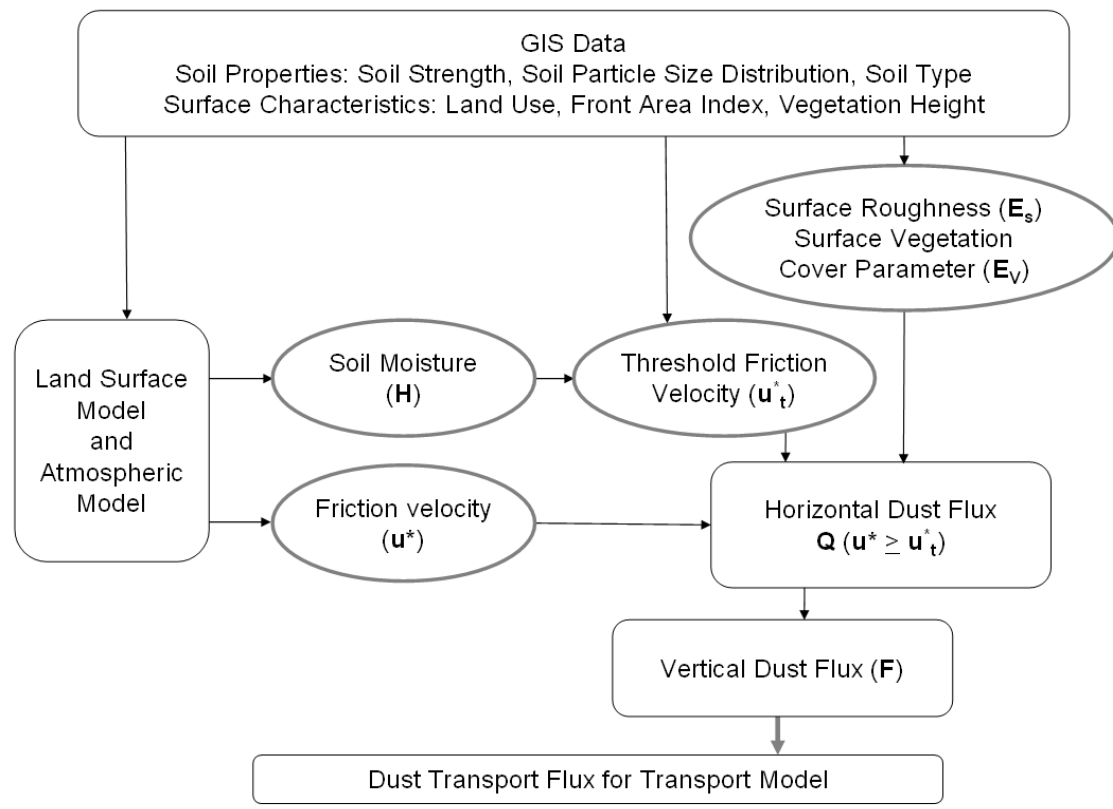
The wind erosion scheme comprises three key parameterizations including  $u_t^*$  (m/s) [57], streamwise sand flux,  $Q$  [58] and the dust emission rate,  $F$  [59] (Figure 2). Six dust particle diameters are considered:  $d \leq 2 \mu\text{m}$ ,  $2 < d \leq 11 \mu\text{m}$ ,  $11 < d \leq 22 \mu\text{m}$ ,  $22 < d \leq 52 \mu\text{m}$ ,  $52 < d \leq 90 \mu\text{m}$ , and  $90 < d \leq 125 \mu\text{m}$ . Next, for each of the  $n$  (6) groups, dust emissions are estimated when  $u^*$  exceeds  $u_t^*$  for a specific dust particle size in a given region. The  $u^*$  is calculated in the MM5 boundary layer scheme while  $u_t^*$  depends on land surface properties as calculated by

$$u_t^* = R \times H \times M \sqrt{\alpha_1 \left( \sigma_p g d + \frac{\alpha_2}{\rho d} \right)} \tag{1}$$

where  $R$  (surface roughness),  $H$  (soil moisture), and  $M$  (soil aggregation) are estimated from soil and vegetation data,  $g$  is gravitational acceleration,  $d$  is the particle’s diameter,  $\sigma_p$  is the ratio of particle density to air density,  $\rho$  is the density of air, and  $\alpha_1$  and  $\alpha_2$  are coefficients [57,60]. The sand flux ( $Q$ ) and dust emissions rate ( $F$ ) are also calculated separately for each particle size group. The main input data for the wind erosion scheme is soil texture; vegetation type and vegetation cover and dust emissions, calculated for erodible lands. Calculating  $u_t^*$  requires soil moisture data, obtained from the LSM, and frontal area surface roughness, which is primarily a function of vegetation. As model simulated soil moisture changes with time, the parameter  $u_t^*$  also varies slowly with time.

IAPS 1.0 uses the OSU LSM, which has a single canopy layer, and the prognostic variables include soil moisture and temperature, water stored in or on the canopy, and snowpack depth and water equivalent. Recently, IAPS1.0 has been applied to the simulation of dust storm events over North China [60].

**Figure 2.** The structure of the IAPS wind-erosion scheme.



IAPS 2.0 couples the meso-scale atmospheric model MM5 and the Unified NOAH land surface model with the wind erosion model, the dust transportation model, the GIS database for land surface characteristics, and a pre-processor for the wind erosion model. The NOAH LSM integrates the diurnally dependent Penman potential evaporation equation, the multilayer soil model, and the primitive canopy layer. This modeling system predicts soil moisture and temperature in four layers (at 10, 30, 60 and 100 cm depth), as well as canopy moisture and water-equivalent snow depth. It also outputs surface and underground run-off accumulations. Compared with the original OSU LSM, many improvements have been achieved for the enhanced representation of physical processes in order to better predict snow depth, snow cover, and frozen soil effects, etc. Differences in the NOAH and OSU land surface models include an increase in the number of soil layers (4 in NOAH, 2 in OSU), changes in the treatment of root zone depth (spatially varying as a function of vegetation in NOAH, fixed value in OSU), as well as improvements in NOAH in the treatment of soil ice, which NOAH estimates based on soil moisture content, soil type, and soil temperature [61–63].

The successful application of modeling systems necessitates full evaluation of modeling systems [64]. Extensive validation has been performed on the modeling components of the modeling systems used in this research, the IAPS 1.0 and IAPS 2.0, including work consistent with published guidelines on model evaluation [64]. The meteorological model, MM5, has been widely evaluated with respect to variables including simulated temperature, relative humidity, height of the planetary boundary layer, and wind speed and direction [65–70]. The OSU land surface model [62,71] and NOAH land surface model has similarly undergone thorough model evaluation [63,72–74].

The impact of land surface processes on the predictive skill of dust storm events was evaluated by using two dust storms in North China (24–25 March 2002 and 21–24 April 2002). The storms were simulated with IAPS 1.0 and IAPS 2.0 and their results were compared. The simulated domain area contains Mongolia, China, the Korean Peninsula and Japan, centered at 40°N and 115°E, with 150 grid cells in longitude and 120 grid cells in latitude, a horizontal resolution of 45 km, and 16 vertical levels. Model initialization and boundary conditions were based on National Centers for Environmental Prediction (NCEP) reanalysis atmospheric data with a horizontal resolution of 2.5° and a one-day spin-up period. NCEP data were interpolated horizontally onto model grid points and then interpolated from pressure levels onto model's vertical levels ( $\sigma$ -levels). The initial values of dust concentration of each particle size group were set to zero. Numerical simulation results were compared and verified with the station observations. The impact of land surface processes on the dust storm simulations was investigated.

### **3. Impact of Land Surface Processes on Dust Storm Simulations**

Active dust storm activity occurred throughout North China in the spring of 2002, with strong dust storm events occurring every 2 to 5 days. In this paper, two typical dust storm episodes, with markedly different weather conditions, dust sources and dust distribution areas, are selected for investigation. While these episodes differ, their characteristics are typical for North China.

### 3.1. Dust Episode of 24–25 March 2002

For the 24–25 March 2002 dust storm event, 850 hPa NCEP reanalysis geopotential height variations at 8:00 Beijing Standard Time (BST) was used, controlled by a southeastward moving cyclone. Prior to this event, a cyclone was moving southeastward from the Lake Baikal area, accompanied by strong northwesterly wind behind the cold front. By 8:00 BST on 25 March the center of the cyclone was located in the vicinity of 122°E, 52°N. Very strong NW and WNW winds occurred behind the cold front, reaching 16 m/s in some areas. This dust episode was mainly limited to northeast China including the eastern regions of Liaoning, Jilin, Hebei and Heilongjiang, with elevated dust levels also observed in Xinjiang and severe dust storms in the eastern Inner Mongolia. Figure 3 shows dust deposition for this storm for observational data [75], and under the IAPS 1.0 and 2.0 modeling systems (Figures 4 and 5), and the difference in average soil moisture simulated by IAPS2.0 and IAPS1.0 (Figure 6). The observational data in Figure 3 and subsequent figures is from the Chinese Sandstorm Almanac [75], developed by the China Meteorological Administration.

**Figure 3.** Distribution of dust affected regions for the 24–25 March 2002 dust-storm event. The red dots indicate the province's capitols; the green lines represent rivers.

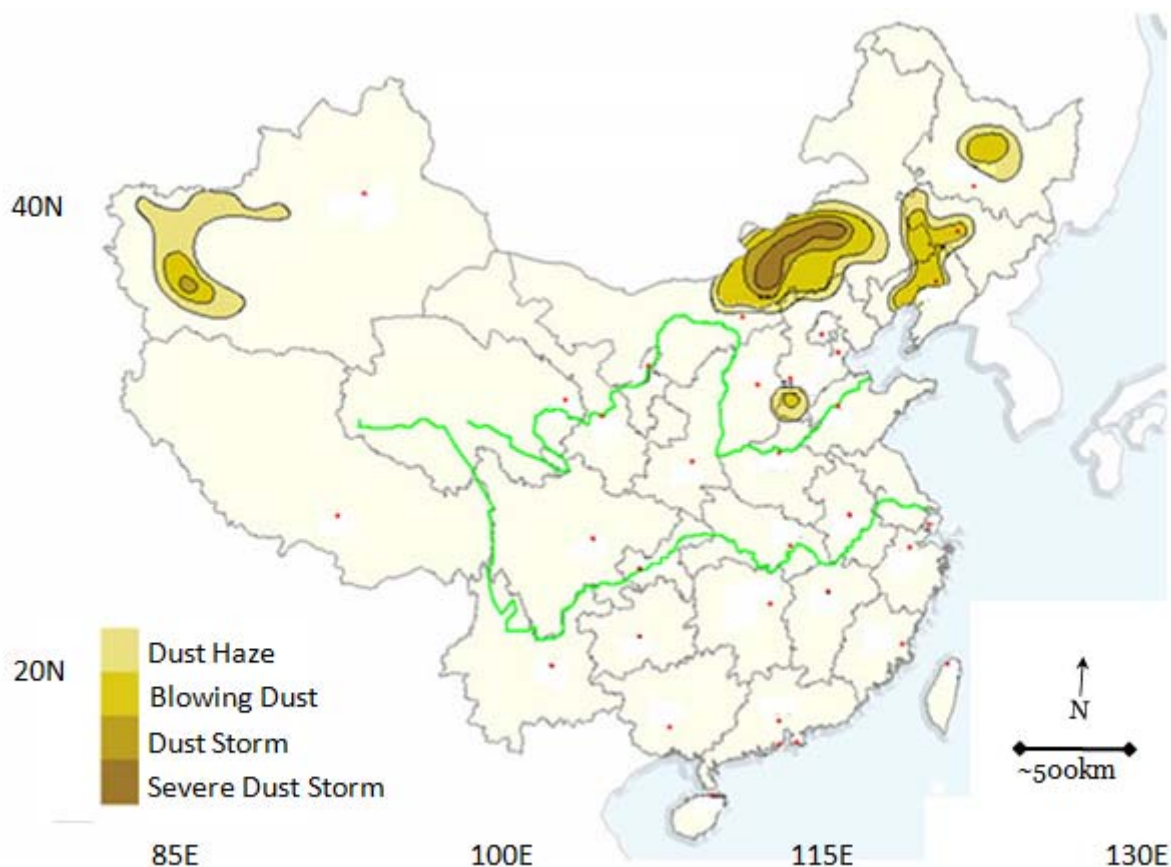


**Figure 4.** Simulations of average dust deposition ( $\text{mg}\cdot\text{m}^{-2}\cdot\text{s}^{-1}$ ) from the 24–25 March 2002 sand-dust storm using IAPS1.0.

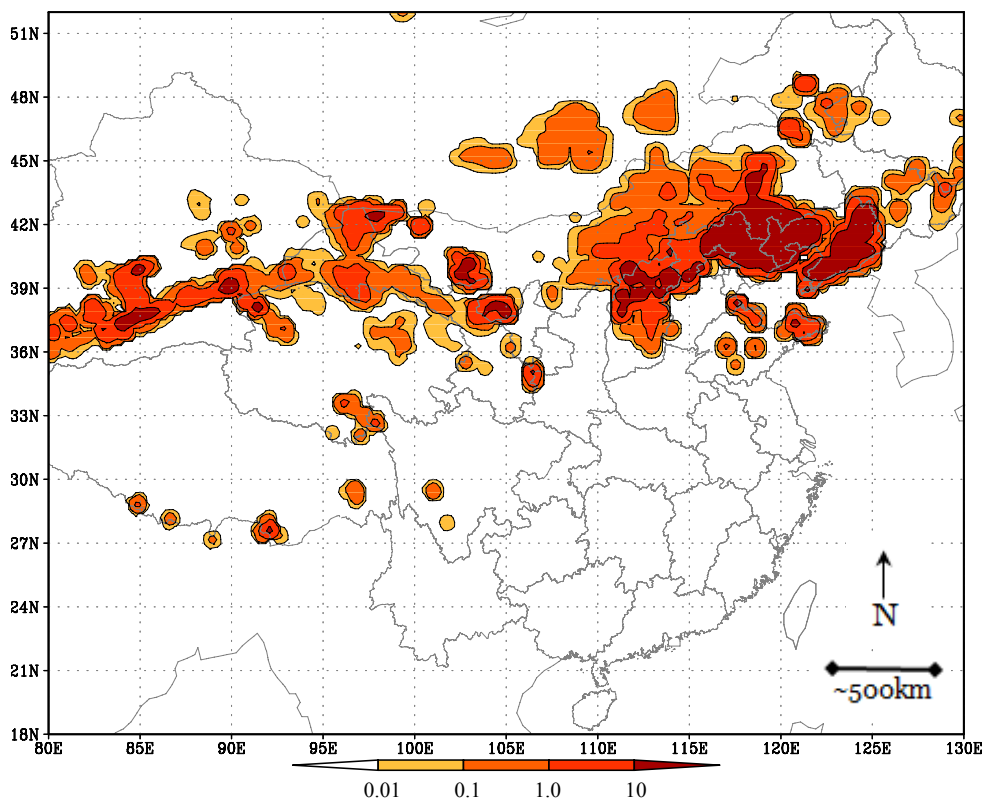


**Figure 5.** Simulations of average dust deposition ( $\text{mg}\cdot\text{m}^{-2}\cdot\text{s}^{-1}$ ) from the 24–25 March 2002 sand-dust storm using IAPS2.0.

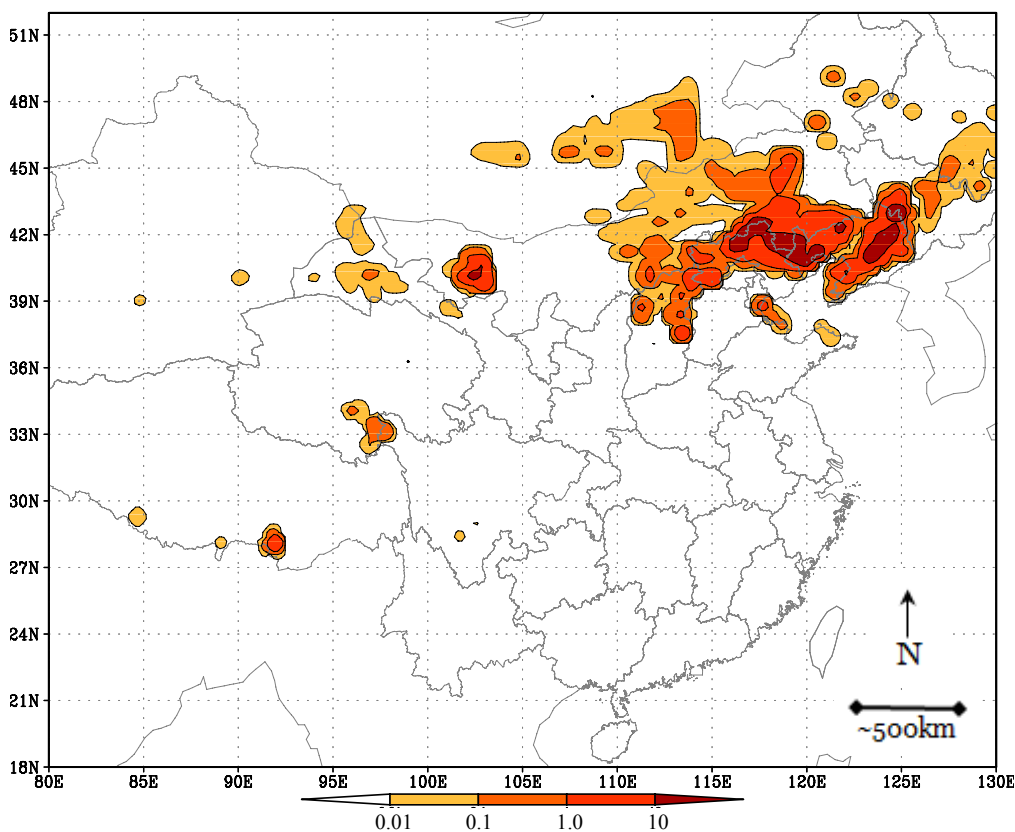
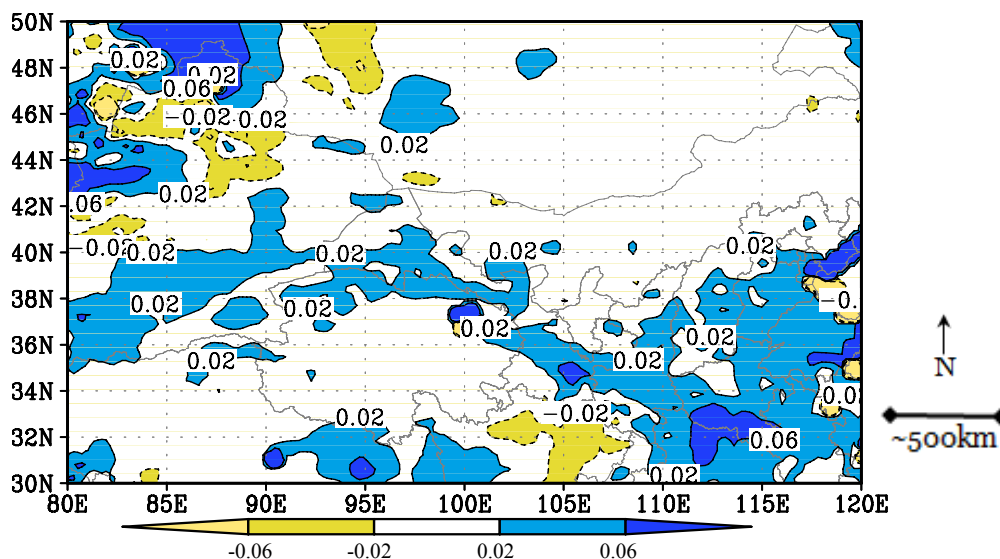


**Figure 6.** Difference in average surface soil moisture ( $\text{g}\cdot\text{cm}^{-3}$ ) simulated by IAPS2.0 and IAPS1.0.



IAPS1.0 dust deposition results generally capture the affected regions noted in observational data, with high deposition estimated for regions that were observed to have severe dust storms, however, large areas not affected by the dust storm are predicted to have high dust deposition, primarily in the central North regions (Figure 4). Dust deposition estimates are improved with IAPS2.0, particularly in eastern China (Figure 5). As shown in Figure 6, IAPS2.0 generally predicts wetter soil moisture than IAPS1.0 in Xinjiang and Gansu which plausibly explain discrepancies between the IAPS1.0 and IAPS2.0 results. The distribution of the difference between  $u^*$  and  $u^*_v$ , which directly represents erodibility, is shown for the IAPS1.0 in Figure 7 and for IAPS2.0 in Figure 8.

**Figure 7.** Overall distribution of the positive value of  $(u^* - u^*_v)$  in the IAPS1.0 simulation.

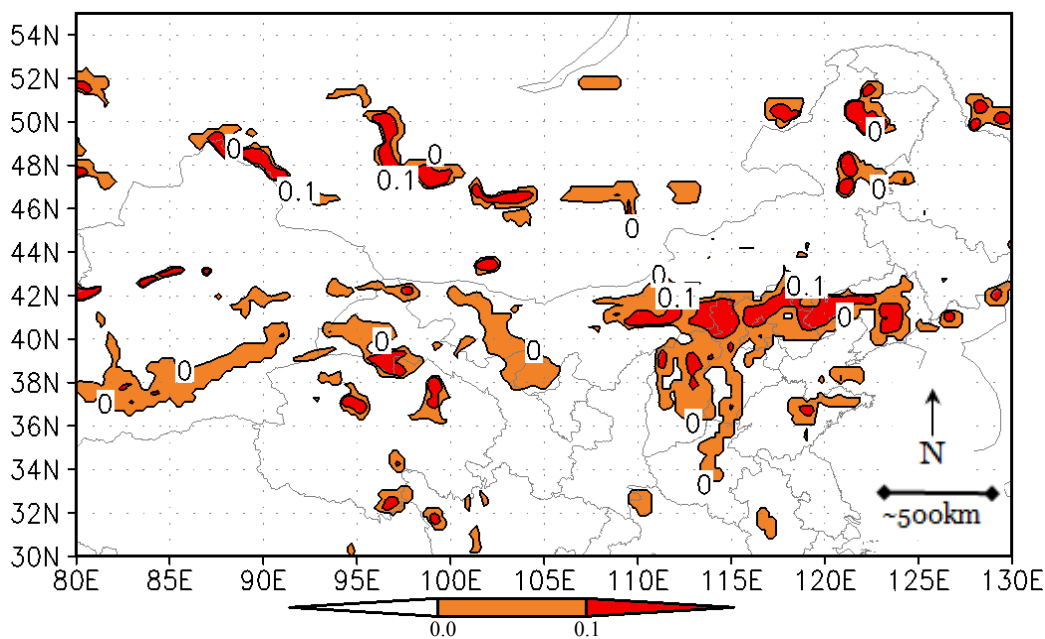
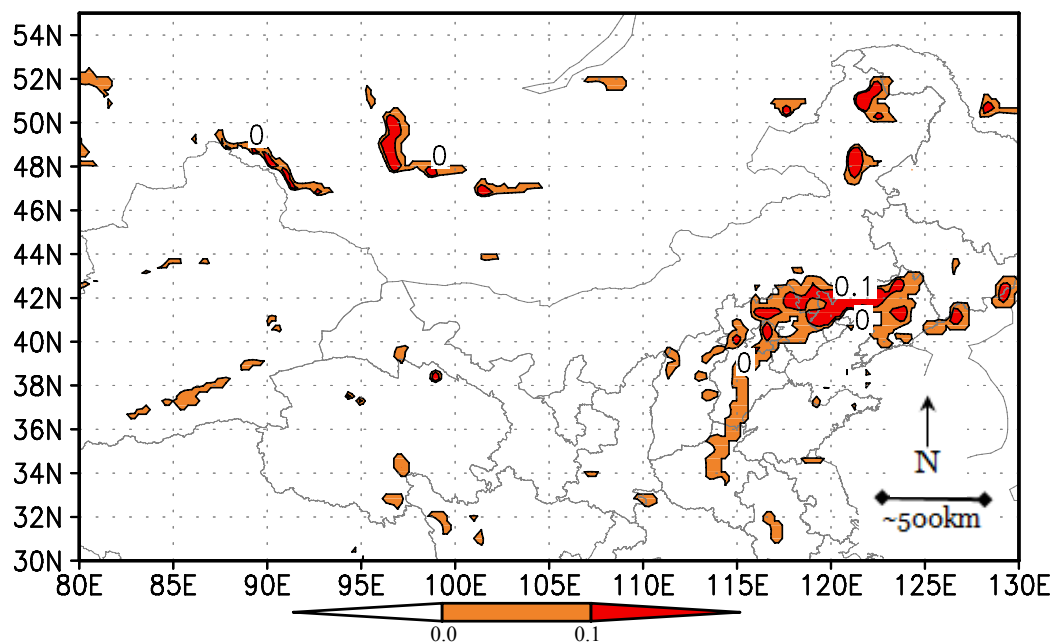


**Figure 8.** Overall distribution of the positive value of  $(u^* - u_i^*)$  in the IAPS2.0 simulation.

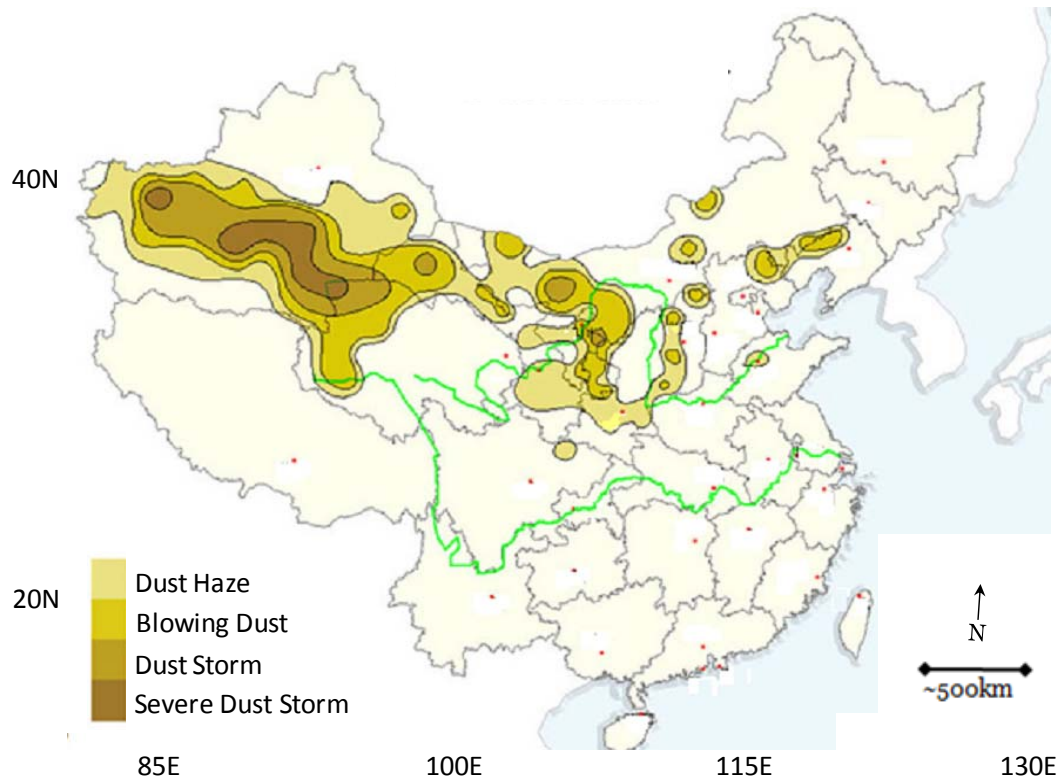


### 3.2. Dust Episode of 21–24 April 2002

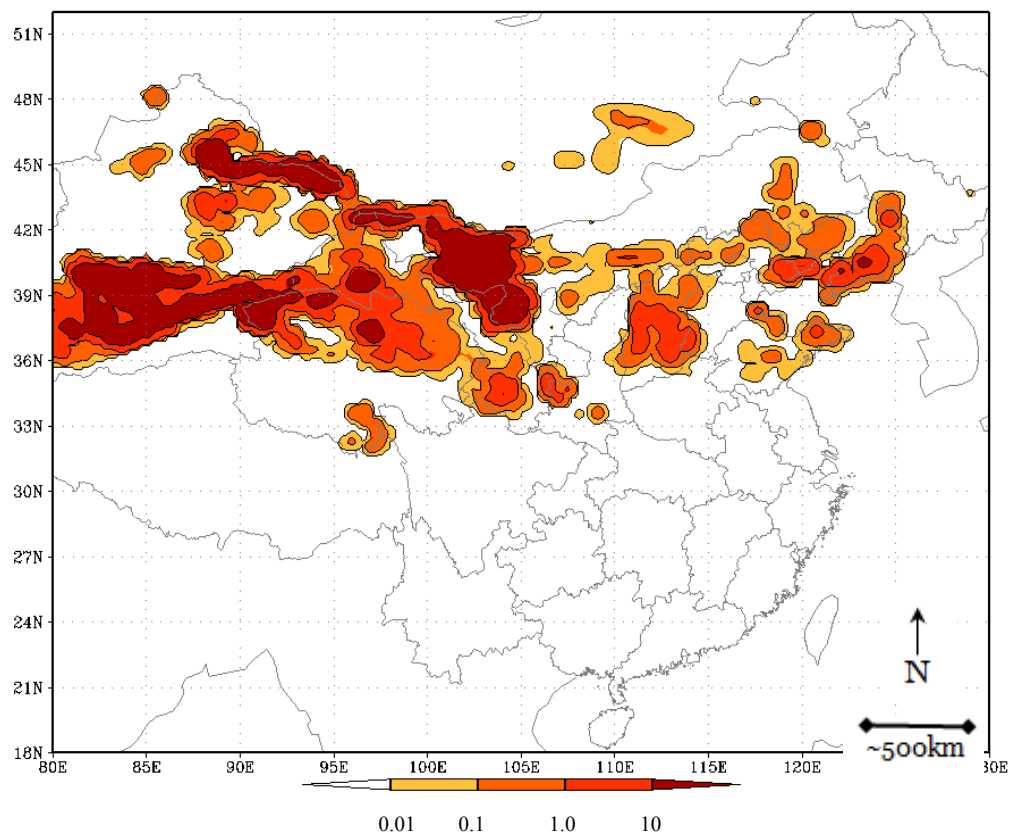
A complicated dust storm event occurred on 21–24 April 2002 in North China, which was affected by a southeastward moving cyclone, a cold front and an anticyclone system. A cyclone, centered at approximately 122°E, 50°N, moved eastward from northeast China, and was accompanied by strong northwesterly wind behind the cold front. By 8:00 BST on 22 April, the center of the cyclone was located in the vicinity of 130°E, 52°N and a high pressure system was present in western Mongolia, with the ridge of high pressure reaching Liaoning. This ridge of high pressure was preceded by very strong SE wind occurred reaching 17–20 m/s in some areas. Next, an anticyclone system centered at approximately 102°E, 45°N formed across the Mongolia-China border. By 8:00 BST on 23 April almost all of North China was affected by this eastward moving anticyclone system. By 8:00 BST on 24 April, the anticyclone system weakened significantly as it moved into central China. Accordingly, dust storms were observed throughout most of northwest China and in some parts of northeast China, as shown in the observational data. Specifically, synoptic records show that from 21–24 April 2002, severe and extensive dust storms affected, Xinjiang, Qinghai, Gansu, Inner Mongolia, Ningxia, Shaanxi, Shanxi, Hebei, Beijing, Tianjin, Liaoning, and Shandong, as shown in observational data (Figure 9). Severe dust storms also occurred in Xinjiang, Inner Mongolia and Ningxia. The spatial distribution of this dust covers a large area. The severe dust deposition is mainly concentrated in northwest China, while a relatively light deposition of dust occurs in northeast China.

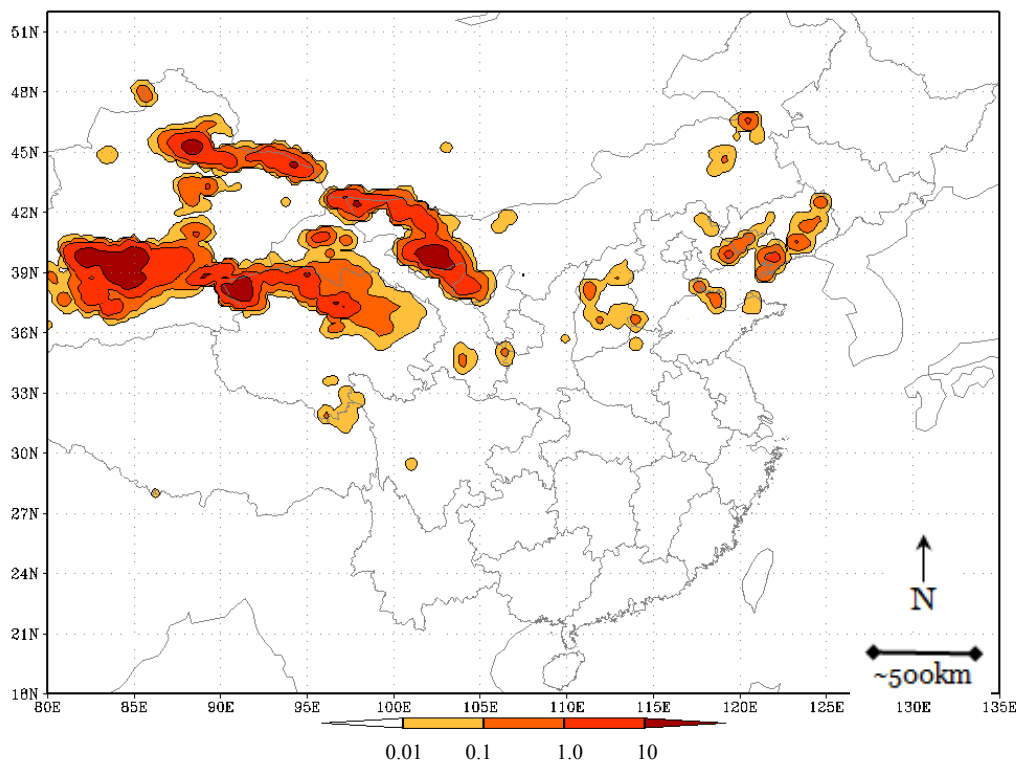
The IAPS1.0 simulation results show the similar patterns as the observational data (Seen from Figure 10). However, the model over-predicts dust storm activity in some regions, particularly in northeast China. The IAPS2.0 results (Figure 11) are similar to those from IAPS1.0, however visual inspection suggests that IAPS2.0 results better match observational data. The simulated dust deposition is higher than observed values for some regions, such as in the western part of Inner Mongolia (around 102°E, 40°N). In the East Liaoning Peninsula (around 122°E, 40°N), a significant dust concentration was simulated, while no dust activities were reported by observational data.

**Figure 9.** Distribution of dust affected regions for the 21–24 April 2002 dust-storm event.



**Figure 10.** Simulations of average dust deposition ( $\text{mg}\cdot\text{m}^{-2}\cdot\text{s}^{-1}$ ) using IAPS 1.0.



**Figure 11.** Simulations of average dust deposition ( $\text{mg}\cdot\text{m}^{-2}\cdot\text{s}^{-1}$ ) using IAPS 2.0.

#### 4. Discussion

The ability to predict the frequency and occurrence of sand storms is a critical policy issue in many parts of the world. As noted by the World Meteorological Association (WMO), sand storms can severely harm human health, disrupt air and transportation systems, alter marine productivity through changes in oceanic nutrient deposition, affect agriculture through soil erosion and harm to crops and livestock, and hinder food and water security [76]. The WMO established the Sand and Dust Storm Warning Advisory and Assessment System (SDS-WAS) to help improve the forecasting of dust storms by encouraging forecasting capabilities and coordinating efforts worldwide [76].

Previous studies have investigated dust storms using a variety of approaches, such as the use of statistical analysis of predictor variables (e.g., monthly temperature anomalies, seasonal and annual precipitation, soil moisture) to generate seasonal forecasts in Inner Mongolia [77]. As another example, statistical analysis was used to estimate sandstorms in the Gansu Province of China [78] and in Iran [79]. Land surface temperature from satellite data were compared to measurements of total suspended particles, finding that land surface temperature may be a useful indicator of storms [80]. Other approaches, more similar to our methods, integrate models based on understanding of physical systems (e.g., meteorological models), rather than statistical models, to estimate dust storms, such as a study by the United States Air Force Weather Agency using the University of Colorado CARMA dust transport model in conjunction with MM5 [81].

#### 5. Conclusions

In efforts to further advance the ability to predict and understand dust storms, we applied an improved IAP dust storm numerical modeling and prediction system (IAPS 2.0) to the prediction of

dust storm events over North China for two typical dust storm episodes with different characteristics with respect to dust sources and the dust affected regions. Results were compared to those generated by the original system (IAPS 1.0). Both modeling systems provided reasonable estimates as gauged by comparison to observational data. However, for both case study events the IAPS 2.0 system was better able to predict dust storm sources and capture dust storm patterns than IAPS 1.0. The use of the NOAH LSM in IAPS 2.0 improves the model performance through comprehensive representation of land surface processes and its interaction with the atmosphere than OSU LSM in the IAPS 1.0. In particular, the use of IAPS 2.0 significantly improves the simulation of soil moisture. This may likely lead to improvements in simulating  $u^*$ , which is a key parameter for surface dust emission.

While the results from IAPS2.0 provided better agreement with observational patterns of dust deposition than did IAPS1.0, results for regions such as western Inner Mongolia (around 102°E, 40°N) and the eastern Liaoning Peninsula (around 122°E, 40°N), were better estimated by the IAPS 1.0. These discrepancies could result from a number of possible factors. Firstly, the geographic information data sets used in the aforementioned prediction system are limited, as it might not capture land use and land cover changes due to anthropogenic or natural factors that have taken place in the past decade, and there still exist uncertainties in critical surface characteristic variables such as soil particle size distribution, soil texture and surface vegetation cover. The NCEP reanalysis data, which was used for the initialization and boundary conditions of the atmospheric model, have a coarser resolution (2.5°) than that of the atmospheric model itself (45 km) and therefore may miss sub-scale heterogeneity. Moreover, initial dust concentration estimates are currently unavailable, and wet deposition may not be fully parameterized in the present IAP 2.0 system. These issues warrant further study.

In summary, this work indicates that the application of the IAPS2.0 model provides significant improvements over the IAPS1.0 modeling system for simulation and prediction of dust storm events in North China. It suggests the reasonable prediction by IAPS2.0 will provide helpful information for the sandstorm risk assessment and disaster reduction. We recommend that future work address the issues described above in order to further improve IAPS2.0 dust estimates. Finally, the link between modeling and decision making should be further strengthened.

## Acknowledgements

This work is jointly supported by the National Basic Research Program of China (Grant No.2009CB421406), and National Key Technologies R&D Program of China (Grant No.2007BAC29B03 and 2008BAC40B02).

## References

1. Gao, T.; Yu, X.; Ma, Q.; Li, H.; Li, X.; Si, Y. Climatology and trends of the temporal and spatial distribution of sandstorms in inner Mongolia. *Water Air Soil Poll.* **2003**, *3*, 51-66.
2. Quan, Q.; Pan, B.; Li, N.; Li, Q.; Zhang, J.; Xu, S.; Gao, H.; Liu, J. Loess record of the evolution history of severe sandstorms in the Tengger Desert during the Last Interglacial Period (MIS5). *Geosciences J.* **2010**, *14*, 155-162.
3. Li, S.; Dong, S.; Zhang, X.; Gao, Z. Assessment of land degradation and its spatial and temporal variation in Beijing surrounding area. *Proc. SPIE* **2005**, doi: 10.1117/12.618799.

4. Liu, X.; Xie, P.; Liu, Z.; Li, T.; Zhong, L.; Xiang, Y. Economic assessment of acute health impact due to inhalable particulate air pollution in the pearl river delta (in Chinese). *Beijing Daxue Xuebao (Ziran Kexue Ban)* **2010**, *46*, 829-834.
5. Pope, C.A., III; Dockery, D.W. Health effects of fine particulate air pollution: Lines that connect. *J. Air Waste Manag. Assoc.* **2006**, *56*, 709-742.
6. Bell, M.L.; Ebisu, K.; Peng, R.D.; Walker, J.; Samet, J.M.; Zeger, S.L.; Dominici, F. Seasonal and regional short-term effects of fine particles on hospital admissions in 202 US counties, 1999–2005. *Am. J. Epidemiol.* **2008**, *168*, 1301-1310.
7. Chen, Y.S.; Sheen, P.C.; Chen, E.R.; Liu, Y.K.; Wu, T.N.; Yang, C.Y. Effects of Asian dust storm events on daily mortality in Taipei, Taiwan. *Environ. Res.* **2004**, *95*, 151-155.
8. Bell, M.L.; Levy, J.K.; Lin, Z. The effect of sandstorms and air pollution on cause-specific hospital admissions in Taipei, Taiwan. *Occup. Environ. Med.* **2008**, *65*, 104-111.
9. Chen, Y.S.; Yang, C.Y. Effects of Asian dust storm events on daily hospital admissions for cardiovascular disease in Taipei, Taiwan. *J. Toxicol. Environ. Health A* **2005**, *68*, 1457-1464.
10. Meng, Z.Q.; Zhang, J.; Geng, H.; Lu, B.; Zhang, Q.X. Influence of dust storms on daily respiratory and circulatory outpatient number (in Chinese). *Zhongguo Huanjing Kexue* **2007**, *27*, 116-120.
11. Yang, C.Y.; Tsai, S.S.; Chang, C.C.; Ho, S.C. Effects of Asian dust storm events on daily admissions for asthma in Taipei, Taiwan. *Inhal. Toxicol.* **2005**, *17*, 817-821.
12. Zhang, M.; Song, Y.; Cai, X.; Zhou, J. Economic assessment of the health effects related to particulate matter pollution in 111 Chinese cities by using economic burden of disease analysis. *J. Environ. Manage.* **2008**, *88*, 947-954.
13. Im, H.J.; Kwon, H.J.; Ha, M.; Lee, S.G.; Hwang, S.S.; Ha, E.H.; Cho, S.H. Public perceptions of the risk of Asian dust storms in Seoul and its metropolitan area. *J. Prev. Med. Public Health* **2006**, *39*, 205-212.
14. Chang, C.C.; Hwang, J.S.; Chan, C.C.; Wang, P.Y.; Cheng, T.J. Effects of concentrated ambient particles on heart rate, blood pressure, and cardiac contractility in spontaneously hypertensive rats during a dust storm event. *Inhal. Toxicol.* **2007**, *19*, 973-978.
15. Lei, Y.C.; Chan, C.C.; Wang, P.Y.; Lee, C.T.; Cheng, T.J. Effects of Asian dust event particles on inflammation markers in peripheral blood and bronchoalveolar lavage in pulmonary hypertensive rats. *Environ. Res.* **2004**, *95*, 1-76.
16. Meng, Z.; Zhang, Q. Damage effects of dust storm PM<sub>2.5</sub> on DNA in alveolar macrophages and lung cells of rats. *Food Chem. Toxicol.* **2007**, *45*, 1368-1374.
17. Batjargal, Z.; Dulam, J.; Chung, Y.S. Dust storms are an indication of an unhealthy environment in East Asia. *Environ. Monit. Assess.* **2006**, *114*, 447-460.
18. Davara, F.; de la Cruz, A. Dust storm monitoring: effects on the environment, human health and potential security conflicts. *Proc. SPIE* **2004**, *5574*, 361-371.
19. Chung, Y.S. On the observations of yellow sand in Korea. *Atmos. Environ.* **1992**, *26A*, 2743-2749.
20. Chon, J. Historical records of yellow sand observations in China. *Res. Environ. Sci.* **1994**, *7*, 1-11.
21. Chung, Y.S.; Kim, H.S.; Judger, D.; Natsagdorj, L.; Chen, S.J. On sand and duststorms and associated significant dust fall observed in Chongju-Cheongwon, Korea during 1997–2000. *Water Air Soil Poll.: Focus.* **2003**, *3*, 5-19.

22. Chung, Y.S.; Kim, H.S.; Park, K.H.; Jhun, J.G.; Chen, S.J. Atmospheric loadings, concentrations and visibility associated with sandstorms: satellite and meteorological analysis. *Water Air Soil Poll.: Focus*. **2003**, *3*, 21-40.
23. Kurosaki, Y.; Mikami, M. Recent frequent dust events and their relation to surface wind in East Asia. *Geophys. Res. Lett.* **2003**, *30*, 1736.
24. Wang, W.; Fang, Z.Y. Numerical simulation and synoptic analysis of dust emission and transport in East Asia. *Glob. Planet. Change* **2006**, *52*, 57-70.
25. Kim, Y.K.; Song, S.K.; Lee, H.W.; Kim, C.H.; Oh, I.B. Characteristics of Asian dust transport based on synoptic meteorological analysis over Korea. *J. Air Waste Manag. Assoc.* **2006**, *56*, 306-316.
26. Kim, H.S.; Chung, Y.S. On the sandstorms and associated airborne dust fall episodes observed at Cheongwon in Korea in 2005. *Air Qual. Atmos. Health*. **2010**, *3*, 83-94.
27. Chung, Y.S. Air pollution detection by satellite: The transport and deposition of air pollutants over oceans. *Atmos. Environ.* **1986**, *20*, 617-630.
28. Kim, J. Transport routes and source regions of Asian dust observed in Korea during the past 40 years (1965–2004). *Atmos. Environ.* **2008**, *42*, 4778-4789.
29. Mckendry, I.G.; Hacker, J.P.; Stull, R. Long-range transport of Asian dust to the Hawaiian Islands. *Science*. **2001**, *220*, 198-197.
30. Chen, Y.; Cai, Q.; Tang, H. Dust storm as an environmental problem in North China. *Environ. Manage.* **2003**, *32*, 413-417.
31. Lee, H.C.; Liu, C.M. Coping with dust storm events: information, impacts and policymaking in Taiwan. *Terr. Atmos. Oceanic Sci.* **2004**, *15*, 1035-1050.
32. Wang, Y.; Stein, A.F.; Draxler, R.R.; de la Rosa, J.D.; Zhang, X. Global sand and dust storms in 2008: observation and HYSPLIT model verification. *Atmos. Environ.* **2011**, *45*, 6368-6381.
33. Chung, Y.S.; Yoon, M.B. On the occurrence of yellow sand and atmospheric loadings. *Atmos. Environ.* **1996**, *30*, 2387-2397.
34. Chung, Y.S.; Kim, H.S.; Dulam, J.; Harris, J. On heavy dust fall observed with explosive sandstorms in Cheongwon-Chongju, Korea in 2002. *Atmos. Environ.* **2003**, *37*, 3425-3433.
35. Chung, Y.S.; Kim, H.S. Observations of massive-air pollution transport and associated air quality in the Yellow Sea region. *Air Quality Atmos. Health* **2008**, *1*, 69-70.
36. Kim, H.S.; Chung, Y.S. Satellite and ground observations for large-scale air pollution transport in the Yellow Sea Region. *J. Atmos. Chem.* **2008**, *60*, 103-116.
37. Ding, R.; Li, J.; Wang, S.; Ren, F. Decadal change of the spring dust storm in northwest China and the associated atmospheric circulation. *Geophys. Res. Lett.* **2005**, *32*, L02808.
38. Kim, Y.S.; Iwasaka, Y.; Shi, G.Y.; Nagatani, T.; Shibata, T.; Trochkin, D.; Matsuki, A.; Yamada, M.; Chen, B.; Zhang, D.; Nagatani, M.; Nakata, H. Dust particles in the free atmosphere over desert areas on the Asian continent: measurements from summer 2001 to summer 2002 with balloon-borne optical particle counter and lidar, Dunhuang, China. *J. Geophys. Res.* **2004**, *109*, D19S26.
39. Wehner, B.; Wiedensohler, A.; Tuch, T.M.; Wu, Z.J.; Hu, M.; Slanina, J.; Kiang, C.S. Variability of the aerosol number size distribution in Beijing, China: New particle formation, dust storms, and high continental background. *Geophys. Res. Lett.* **2004**, *31*, 1-4.

40. Wu, X.; Zheng, X.; Li, X.; Liu, J.; Kang, L.; Jiang, X. Analyses on the characteristics and weather pattern classifications of East-Asia spring dust storms by using meteorological satellite images (in Chinese). *Climatic Environ. Res.* **2004**, *9*, 1-13.
41. Qian, W.H.; Quan, L.S.; Shi, S.Y. Variations of the dust storm in China and its climatic control. *J. Climate* **2002**, *15*, 1216-1229.
42. Lin, Z.; Chen, H.; Zhang, S.; Xu, X. Climatic and environmental background for the anomalous spring sandstorms over the North China during 2003 (in Chinese). *Climatic Environ. Res.* **2004**, *9*, 191-202.
43. Fan, K.; Wang, H.J. Antarctic oscillation and the dust weather frequency in North China. *Geophys. Res. Lett.* **2004**, *31*, L10201.
44. In, H.J.; Park, S.U. Estimation of dust emission amount for a dust storm event occurred in April 1998 in China. *Water Air Soil Poll.* **2003**, *148*, 201-221.
45. Shao, Y. Simplification of a dust emission scheme and comparison with data. *J. Geophys. Res.* **2004**, *109*, D10202, 1-6.
46. Shen, Y.; Shen, Z.; Du, M.; Wang, W. Dust emission over different land surface in the arid region of Northwest China. *J. Meteorol. Soc. Jpn.* **2005**, *83*, 935-942.
47. Song, Z. A numerical simulation of dust storms in China. *Environ. Model. Softw.* **2004**, *19*, 141-151.
48. Zhang, X.L.; Cheng, L.; Chung, Y.S. Development of a severe sand-dust storm model and its application to Northwest China. *Water Air Soil Poll.* **2003**, *3*, 173-190.
49. Zhang, X.Y.; Gong, S.L.; Zhao, T.L.; Arimoto, R.; Wang, Y.O.; Zhou, Z.J. Sources of Asian dust and role of climate change versus desertification in Asian dust emission. *Geophys. Res. Lett.* **2003**, *30*, 2272.
50. Gong, S.L.; Zhang, X.Y.; Zhao, T.L.; McKendry, I.G.; Jaffe, D.A.; Lu, N.M. Characterization of soil dust aerosol in China and its transport and distribution during 2001 ACE-Asia: 2. Model simulation and validation. *J. Geophys. Res.* **2003**, *108*, 4262.
51. Wang, L.; Zhao, L.; Shou, S.; Wang, J. Observation and Numerical Simulation Analysis of the Severe Sand Storm over Northern China in April of 2009 (in Chinese). *Meteorol. Month.* **2011**, *37*, 309-317.
52. Sun, J.; Zhao, L.; Zhao, S. A numerical simulation on severe dust storm events in North China and their dust sources (in Chinese). *Climatic Environ. Res.* **2004**, *9*, 139-154.
53. Chen, F.; Dudhia, J. Coupling an advanced land surface-hydrology model with the Penn-State National Center for Atmospheric Research (NCAR) MM5 modeling system. Part I: Model implementation and sensitivity. *Mon. Weather Rev.* **2001**, *129*, 569-585.
54. Chen, F.; Dudhia, J. Coupling an advanced land surface-hydrology model with the Penn-State NCAR MM5 modeling system. Part II: preliminary model validation. *Mon. Weather Rev.* **2001**, *129*, 587-604.
55. Mitchell, K. *The Community NOAA Land-Surface Model (LSM) User's Guide*; Public Release Version 2.7.1; National Weather Service, National Center for Environmental Prediction: Camp Springs, MD, USA, 2005.

56. Dudhia, J.; Gill, D.; Manning, K.; Wang, W.; Bruyere, C. *PSU/NCAR Mesoscale Modeling System Tutorial Class Notes and Users' Guide*; MM5 Modeling System Version 3; NCAR: Boulder, CO, USA, 2005.
57. Shao, Y.; Lu, H. A simple expression for wind erosion threshold friction velocity. *J. Geophys. Res.* **2000**, *105*, 22437-22443.
58. Owen, R.P. Saltation of uniform grains in air. *J. Fluid Mech.* **1964**, *20*, 225-242.
59. Shao, Y. A model for mineral dust emission. *J. Geophys. Res.* **2001**, *106*, 20239-20254.
60. Sun, J.; Zhao, L.; Zhao, S.; Zhang, R. An integrated dust storm prediction system suitable for East Asia and its simulation results. *Global Planet. Change* **2006**, *52*, 71-87.
61. De Haan, L.L.; Kanamitsu, M.; Lu, C.H.; Roads, J.O. A comparison of the Noah and OSU land surface models in the ECPC seasonal forecast model. *J. Hydrometeorol.* **2007**, *8*, 1031-1048.
62. Sridhar, V.; Elliott, R.L.; Chen, F.; Brotzge, J.A. Validation of the NOAA-OSU land surface model using surface flux measurements in Oklahoma. *J. Geophys. Res.* **2002**, *107*, 4418.
63. Ek, M.B.; Mitchell, K.E.; Lin, Y.; Rogers, E.; Grunmann, P.; Koren, V.; Gayno, G.; Tarpley, J.D. Implementation of Noah land surface model advances in the National Centers for Environmental Prediction operational mesoscale Eta model. *J. Geophys. Res.* **2003**, *108*, 8851.
64. Jakeman, A.J.; Letcher, R.A.; Norton, J.P. Ten iterative steps in development and evaluation of environmental models. *Environ. Model. Softw.* **2006**, *21*, 602-614.
65. Colle, B.A.; Olson, J.B.; Tongue, J.S. Multiseason verification of the MM5. Part I: Comparison with the Eta model over the central and Eastern United States and impact of MM5 resolution. *Weather Forecast.* **2003**, *18*, 431-457.
66. Colle, B.A.; Olson, J.B.; Tongue, J.S. Multiseason verification of the MM5. Part II: Evaluation of high-resolution precipitation forecasts over the Northeastern United States. *Weather Forecast.* **2003**, *18*, 458-480.
67. Dudhia, J.; Bresch, J. A Global Version of MM5: Method and Verification. In *Proceedings of 20th Conference on Weather Analysis and Forecasting/16th Conference on Numerical Weather Prediction*, Seattle, WA, USA, 12–16 January 2004; pp. 3259-3262.
68. Zhang, Y.; Liu, P.; Pun, B.; Seigneur, C. A comprehensive performance evaluation of MM5-CMAQ for the Summer 1999 Southern Oxidants Study episode-Part I: Evaluation protocols, databases, and meteorological predictions. *Atmos. Environ.* **2006**, *40*, 4825-4838.
69. Zhang, Y.; Liu, P.; Pun, B.; Seigneur, C. A comprehensive performance evaluation of MM5-CMAQ for the summer 1999 southern oxidants study episode, Part III: Diagnostic and mechanistic evaluations. *Atmos. Environ.* **2006**, *40*, 4856-4873.
70. Han, Z.; Ueda, H.; An, J. Evaluation and intercomparison of meteorological predictions by five MM5-PBL parameterizations in combination with three land-surface models. *Atmos. Environ.* **2008**, *42*, 233-249.
71. Chen, F.; Mitchell, K.; Schaake, J.; Xue, Y.; Pan, H.L.; Koren, V.; Duan, Q.Y.; Ek, M.; Betts, A. 1996: Modeling of land surface evaporation by four schemes and comparison with FIFE observations. *J. Geophys. Res.* **1996**, *101*, 7251-7268.
72. Decharme, B. Influence of runoff parameterization on continental hydrology: Comparison between the Noah and the ISBA land surface models. *J. Geophys. Res.* **2007**, *112*, D19108.

73. Hogue, T.S.; Bastidas, L.; Gupta, H.; Sorooshian, S.; Mitchell, K.; Emmerich, W. Evaluation and transferability of the Noah land surface model in semiarid environments. *J. Hydrometeorol.* **2005**, *6*, 68-84.
74. Tewari, M.; Chen, F.; Wang, W.; Dudhia, J.; LeMone, M.A.; Mitchell, K.; Ek, M.; Gayno, G.; Wegiel, J.; Cuenca, R.H. Implementation and Verification of the Unified NOAA Land Surface Model in the WRF Model. In *Proceedings of 20th Conference on Weather Analysis and Forecasting/16th Conference on Numerical Weather Prediction*, Seattle, WA, USA, 12–16 January 2004; pp. 2165-2170.
75. Niu, R. *Sand-Dust Weather Almanac* (in Chinese); Meteorological Press: Beijing, China, 2004.
76. WHO Secretariat. *WMO Sand and Dust Storm Warning Advisory and Assessment System (SDWAS) Science and Implementation Plan in 2011–2015*; WMO: Geneva, Switzerland, 2011.
77. Gao, T.; Zhang, X.; Li, Y.; Wang, H.; Xiao, S.; Wulan; Teng, Q. Potential predictors for spring season dust storm forecast in Inner Mongolia, China. *Theor. Appl. Climatol.* **2009**, *97*, 255-263.
78. Dong, J.; Chen, H.; Wang, J.; Sun, D. Sandstorm occurrence frequency short-term prediction based on bootstrap method. *Lect. Notes Comput. Sci.* **2008**, *5370*, 571-580.
79. Jamalizadeh, M.R.; Moghaddamnia, A.; Piri, J.; Arbabi, V.; Homayounifar, A.; Shahrwyari, A. Dust storm prediction using ANNs technique: A case study—Zabol City. *World Acad. Sci. Eng. Tech.* **2008**, *43*, 512-520.
80. Liu, Z.; Ma, J.; Han, X.; Zhang, X. The comparison analysis of AVHRR LST data and TSF data in dust sources region: A case study during strong dust storm of Spring-Summer in 2001. *Proc. SPIE* **2003**, *5286*, 356-358.
81. Barnun, B.H.; Winstead, N.S.; Wesely, J.; Hakola, A.; Colarco, P.R.; Toon, O.B.; Ginoux, P.G.; Brooks, L.; Hasselbarth, B.T. Forecasting dust storms using the CARMA-dust model and MM5 weather data. *Environ. Model. Softw.* **2004**, *19*, 129-140.

© 2012 by the authors; licensee MDPI, Basel, Switzerland. This article is an open access article distributed under the terms and conditions of the Creative Commons Attribution license (<http://creativecommons.org/licenses/by/3.0/>).